

Revisiting Nuclear Quadrupole Moments in $^{39-41}\text{K}$ Isotopes

Yashpal Singh ^{*}, D. K. Nandy and B. K. Sahoo [†]

Theoretical Physics Division, Physical Research Laboratory, Navrangpura, Ahmedabad - 380009, India

Nuclear quadrupole moments (Q s) in three isotopes of potassium (K) with atomic mass numbers 39, 40 and 41 are evaluated more precisely in this work. The Q value of ^{39}K is determined to be $0.0614(6)$ b by combining the available experimental result of the electric quadrupole hyperfine structure constant (B) with our calculated B/Q result of its $4P_{3/2}$ state. Furthermore combining this Q value with the measured ratios $Q(^{40}\text{K})/Q(^{39}\text{K})$ and $Q(^{41}\text{K})/Q(^{39}\text{K})$, we obtain $Q(^{40}\text{K}) = -0.0764(10)$ b and $Q(^{41}\text{K}) = 0.0747(10)$ b , respectively. These results disagree with the recently quoted standard values in the nuclear data table within the given uncertainties. The calculations are carried out by employing the relativistic coupled-cluster theory at the singles, doubles and involving important valence triples approximation. The accuracies of the calculated B/Q results can be viewed on the basis of comparison between our calculated magnetic dipole hyperfine structure constants (A s) with their corresponding measurements for many low-lying states. Both A and B results in few more excited states are presented for the first time.

PACS numbers: 21.10.Ky, 31.15.aj, 31.30.Gs, 32.10.Fn

I. INTRODUCTION

Potassium (K) atom has three naturally abundant isotopes with atomic mass numbers 39, 40 and 41. Using the modern femtosecond laser frequency combs and polarization quantum-beat techniques, high precision measurements of hyperfine structure constants in $4P$ and $3D$ states are carried out [1, 2]. Also, a number of measurements of these quantities were carried out in the ground and other states long ago using the atomic beam magnetic resonance and level crossing techniques (e.g. see review article by Arimondo *et al.* [3]). Theoretical studies of these quantities are of immense interest to atomic physicists to test the accuracies of the wave functions in the nuclear region [4–6]. However, theoretical evaluation of these quantities require atomic calculations and nuclear moments [4, 5, 7, 8]. Nuclear magnetic moments (μ s) of the above K isotopes are known very precisely and the reported results from various studies matches reasonably well with each other [9]. On the other hand, the reported nuclear quadrupole moments (Q s) from various works on these isotopes differ significantly. For example, Q value of ^{39}K is reported as $0.07(2)$ b [10], $0.049(4)$ b [3], $0.0601(15)$ b [11] and 0.0585 b within one percent error [12]. The latest result, $0.0585(6)$ b , is now considered as the standard Q value for ^{39}K [9, 13]. Accurate knowledge of Q values of these isotopes are useful in many applications. These information are interesting in order to test the potential of nuclear models [14, 15], acquiring information about local symmetry [16], to find out asymmetry parameters in nuclei [17, 18], for studying the Mossbauer spectroscopy for the structural determination of the element containing solid state compounds [19] etc.

In this paper, we analyze the electric quadrupole hy-

perfine structure constants for many states in K and report precise Q values of its above mentioned isotopes. As discussed later, we find the new values to be larger than the considered standard values in the literature. Atomic wave functions are calculated using relativistic coupled-cluster (RCC) method in the Fock-space representation and matrix elements of the hyperfine interaction Hamiltonians are estimated using these wave functions in the considered atom.

The rest of the paper is organized as follows: In the next section, we present briefly the theory of hyperfine structure in an atomic system and the single particle matrix elements of the interaction Hamiltonians which are used to evaluate the hyperfine structure constants. In Sec III, we explain the RCC method little elaborately for the calculation of atomic wave functions. Then, we present the results and their discussions before summarizing the work. Unless stated otherwise, we use atomic unit (au) throughout this paper.

II. THEORY OF HYPERFINE STRUCTURE

The hyperfine structures of energy levels in an atom arise due to the interaction between electron angular momenta with the nuclear spin. Details of this theory is given by C. Schwartz in a classic paper [20]. Mathematically, the hyperfine interaction Hamiltonian is given in a general form as non-central interaction between electrons and the nucleus in terms of tensor operators as

$$H_{hfs} = \sum_k T_e^{(k)} \cdot T_n^{(k)}, \quad (2.1)$$

where $T_e^{(k)}$ and $T_n^{(k)}$ are the spherical tensor operators of rank k in the space of electronic and nuclear coordinates, respectively. In the first order perturbation theory, the hyperfine interaction energy W_F of hyperfine state $|F; IJ\rangle$ with total angular momentum $F = I + J$ for I

^{*}Email: yashpal@prl.res.in

[†]Email: bijaya@prl.res.in

and J being the nuclear spin and electronic angular momentum of the associated fine structure state $|J, M_J\rangle$, respectively, taking up to $k = 2$ is given by

$$W_F = \frac{1}{2}AR + B \frac{\frac{3}{2}R(R+1) - 2I(I+1)J(J+1)}{2I(2I-1)2J(2J-1)}, \quad (2.2)$$

with $R = F(F+1) - I(I+1) - J(J+1)$, and A and B are known as the magnetic dipole and electric quadrupole hyperfine structure constant for $k = 1$ and $k = 2$, respectively. The advantage of expressing the change in energy in this form is it separates out the electronic and nuclear factors for which the calculations can be carried out in a simple approach. Here A and B are given by [20, 21]

$$A = \mu_N g_I \frac{\langle J || T_e^{(1)} || J \rangle}{\sqrt{J(J+1)(2J+1)}}, \quad (2.3)$$

and

$$B = Q \left\{ \frac{8J(2J-1)}{(2J+1)(2J+2)(2J+3)} \right\} \langle J || T_e^{(2)} || J \rangle. \quad (2.4)$$

In the above expressions, μ_N and $g_I = \mu/I$ are the nuclear magneton and gyromagnetic ratio, respectively. Since our intention is to verify accuracies of Q values, we estimate B/Q results in this work.

The reduced matrix elements of the electronic spherical tensor operators, $T_e^{(k)} = \sum t_e^{(k)}$, in terms of single orbitals are given by [20, 21]

$$\langle \kappa_f || t_e^{(1)} || \kappa_i \rangle = -(\kappa_f + \kappa_i) \langle -\kappa_f || C^{(1)} || \kappa_i \rangle \int_0^\infty dr \frac{P_f Q_i + Q_f P_i}{r^2} \quad (2.5)$$

and

$$\langle \kappa_f || t_e^{(2)} || \kappa_i \rangle = -\langle \kappa_f || C^{(2)} || \kappa_i \rangle \int_0^\infty dr \frac{P_f Q_i + Q_f P_i}{r^3} \quad (2.6)$$

where κ_i and $P_i(Q_i)$ are the relativistic angular momentum quantum number and large (small) component of Dirac spinor for the corresponding orbital i , respectively. The reduced matrix elements of Racah tensors ($C^{(k)}$) are given by [22]

$$\langle \kappa_f || C^{(k)} || \kappa_i \rangle = (-1)^{j_f+1/2} \sqrt{(2j_f+1)(2j_i+1)} \times \left\{ \begin{matrix} j_f & k & j_i \\ 1/2 & 0 & 1/2 \end{matrix} \right\} \pi(\ell_f, k, \ell_i) \quad (2.7)$$

with the angular momentum selection rule $\pi(\ell_f, k, \ell_i) = 1$ when $\ell_f + k + \ell_i = \text{even}$ for the orbital angular momentum ℓ_f and ℓ_i ; otherwise it is zero.

III. METHODS FOR CALCULATIONS

A. Single particle orbital generation

Accurate generation of atomic orbitals in the nuclear region is very important for the present study. We

TABLE I: Used ζ and ν parameters for different ' ℓ ' symmetries to construct GTOs.

	s	p	d	f	g
ζ	0.0002	0.0004	0.0003	0.0005	0.0004
ν	1.917	1.79	1.77	1.76	1.75

consider here Gaussian type of orbitals (GTOs) which provide natural description of relativistic wave-functions within nucleus [23–25] as basis to construct the mean-field orbitals in the Dirac(Hartree)-Fock (DF) approach. Kinetic balanced condition between the large and small components of Dirac spinor are imposed to ensure correct non-relativistic behavior of the orbitals [25, 26]. GTOs to construct an orbital at a particular location r_i are defined as

$$F^{L(S)}(r_i) = \sum_k \mathcal{N}_k^{L(S)} r_i^{l+1} e^{-\eta_k r_i^2} \quad (3.1)$$

where $L(S)$ represents for large (small) component, k denotes number of GTOs, \mathcal{N} correspond to normalization factor for each GTO and η_k is an arbitrary parameter which has to be chosen suitably for orbitals from different ℓ symmetries. To get more flexibility in optimization of our basis sets, we use the even tempering condition by defining two more parameters ζ and ν as

$$\eta_k = \zeta \nu^{k-1}. \quad (3.2)$$

The radial grid points r_i are defined as

$$r_i = r_0 [e^{h(i-1)} - 1], \quad (3.3)$$

with r_0 is the starting radial function taken inside the nucleus to be 2×10^{-6} at which the wave functions become finite and h is a step size which is defined by taking maximum radial function r_{max} as 150.0 au and total grid points 1000.

We have considered 40 GTOs for each l symmetry orbitals and the considered ζ and ν are given in Table I for different l values. Due to limitation over computational resources and negligible contributions from the high lying virtual orbitals, we have taken up to 24 orbitals from s, p, d symmetries and 17 orbitals from f, g symmetries to construct active space for RCC calculations.

Also, the orbitals are generated by accounting the finite size of the nucleus assuming a two-parameter Fermi-nuclear-charge distribution given by

$$\rho(r_i) = \frac{\rho_0}{1 + e^{(r_i - c)/a}}, \quad (3.4)$$

where ρ_0 is the density for the point nuclei, c and a are the half-charge radius and skin thickness of the nucleus. These parameters are chosen as

$$a = 2.3/4(\ln 3) \quad (3.5)$$

and

$$c = \sqrt{\frac{5}{3} r_{rms}^2 - \frac{7}{3} a^2 \pi^2}, \quad (3.6)$$

where r_{rms} is the root mean square radius of the corresponding nuclei which is taken as 3.61 fm [27].

B. Calculation of atomic wave functions

To calculate matrix elements of the hyperfine interaction Hamiltonian, we use the RCC method where we define atomic wave functions for the considered states with valence orbital denoted by v as [28, 29]

$$|\Psi_v\rangle = e^T \{1 + S_v\} |\Phi_v\rangle, \quad (3.7)$$

where the DF wave function $|\Phi_v\rangle$ is constructed as $|\Phi_v\rangle = a_v^\dagger |\Phi_0\rangle$ with $|\Phi_0\rangle$ is the DF wave function for the closed-shell configuration $[3p^6]$ in the considered K atom. In the above expression, T and S_v are the excitation operators that accounts for core and core-valence correlations to all orders, respectively. Since K is a small size atom, hence correlation effects among electrons are expected to be less. Therefore role of the higher order configurations in determining atomic wave-function could be negligible. On the other-hand consideration of these configurations are computationally very expensive. Owing to this fact we account only all possible single and double configuration excitations to all orders (known as CCSD method) by expressing the above operators in the Fock space representation as

$$T = T_1 + T_2 = \sum_{a,p} a_p^\dagger a_a t_a^p + \frac{1}{4} \sum_{ab,pq} a_p^\dagger a_q^\dagger a_b a_a t_{ab}^{pq} \quad (3.8)$$

$$S_v = S_{1v} + S_{2v} = \sum_{a,p} a_p^\dagger a_v s_v^p + \frac{1}{2} \sum_{ab,pq} a_p^\dagger a_q^\dagger a_b a_v s_{vb}^{pq} \quad (3.9)$$

where the $(a, b, c \dots)$, $(p, q, r \dots)$ and (v) subscripts of the second quantized operators represents core (hole), particle (virtual) and valance orbitals, respectively. However expanding Eq. (3.7) using these CCSD operators to all non-linear terms give rises contributions from higher excitations. We determine the above t and s_v coefficients which correspond to the excitation amplitudes using the following equations

$$\langle \Phi^L | \{\widehat{H_N e^T}\} | \Phi_0 \rangle = 0 \quad (3.10)$$

and

$$\begin{aligned} \langle \Phi_v^L | \{\widehat{H_N e^T}\} S_v | \Phi_v \rangle &= -\langle \Phi_v^L | \{\widehat{H_N e^T}\} | \Phi_v \rangle \\ &+ \langle \Phi_v^L | S_v | \Phi_v \rangle \Delta E_v, \end{aligned} \quad (3.11)$$

with the superscript L(=1,2) representing the single and double excited configurations from the corresponding DF states, the wide-hat symbol denotes the linked terms, ΔE_v is the attachment energy of the valence electron

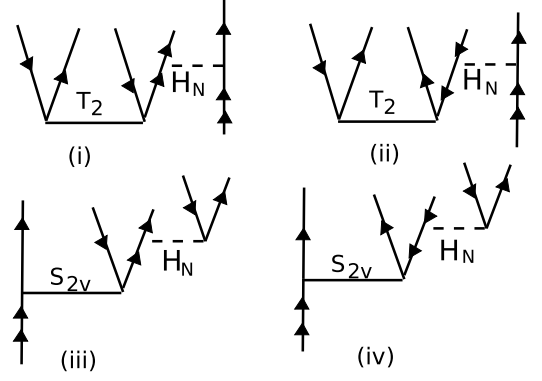


FIG. 1: Typical Goldstone diagrams representing leading-order triple excitations over the CCSD method. Double arrows in the diagrams represents valence electron v , and the lines with upward (downward) arrows represents particle (hole) orbitals.

v and H_N denotes the normal ordering atomic Dirac-Coulomb Hamiltonian H which is taken as

$$H = \sum_i [c\alpha_i \cdot \mathbf{p}_i + (\beta_i - 1)c^2] + \sum_{i \geq j} \frac{1}{r_{ij}}, \quad (3.12)$$

where α and β are usual Dirac matrices, c is the velocity of light. ΔE_v is evaluated by

$$\Delta E_v = \langle \Phi_v | \{\widehat{H_N e^T}\} \{1 + S_v\} | \Phi_v \rangle. \quad (3.13)$$

To improve the quality of energy and calculation of wave functions due to the dominant triple excitations containing the valence orbital, we define a perturbation operator S_{3v} by contracting H_N with T_2 and S_{2v} operators as

$$S_{3v}(s_{vbc}^{pqr}) = \frac{\widehat{H_N T_2} + \widehat{H_N S_{2v}}}{\epsilon_p + \epsilon_q + \epsilon_r - \epsilon_b - \epsilon_c - \epsilon_v}, \quad (3.14)$$

with s_{vbc}^{pqr} correspond to excitation amplitudes and ϵ_i is the DF energy of the electron in the i^{th} orbital. This operator is considered as a part of S_v operator in Eq. (3.13) to get additional contribution to ΔE_v . Since ΔE_v is involved in Eq. (3.11), we solve both the equations simultaneously in an iterative procedure. This approach is generally referred as CCSD(T) method [30]. The diagrammatic representation of these excitations are shown in Fig. 1.

The expectation values due to the hyperfine interaction operators have been evaluated using our RCC method by

$$\begin{aligned} \langle T_e^{(k)} \rangle &= \frac{\langle \Psi_v | T_e^{(k)} | \Psi_v \rangle}{\langle \Psi_v | \Psi_v \rangle} \\ &= \frac{\langle \Phi_v | \{1 + S_v^\dagger\} \overline{T_e^{(k)}} \{1 + S_v\} | \Phi_v \rangle}{\{1 + S_v^\dagger\} \overline{N_0} \{1 + S_v\}} \\ &= \frac{\langle \Phi_v | \{1 + S_{1v}^\dagger + S_{2v}^\dagger\} \overline{T_e^{(k)}} \{1 + S_{1v} + S_{2v}\} | \Phi_v \rangle}{\{1 + S_{1v}^\dagger + S_{2v}^\dagger\} \overline{N_0} \{1 + S_{1v} + S_{2v}\}} \end{aligned} \quad (3.15)$$

where $\overline{T}_e^{(k)} = (e^{T^\dagger} T_e^{(k)} e^T)$ and $\overline{N}_0 = e^{T^\dagger} e^T$. Generally, both $\overline{T}_e^{(k)}$ and \overline{N}_0 in our RCC approach are non-terminating series. These terms are terminated keeping terms minimum up to fourth order in perturbation. Description of this procedure has been given in the previous works [31–33]. Contributions from normalization of the wave functions (*Norm*) are estimated explicitly in the following way

$$Norm = \langle \Psi_v | T_e^{(k)} | \Psi_v \rangle \left\{ \frac{1}{1 + N_v} - 1 \right\} \quad (3.16)$$

where $N_v = \{1 + S_{1v}^\dagger + S_{2v}^\dagger\} \overline{N}_0 \{1 + S_{1v} + S_{2v}\}$.

IV. RESULTS AND DISCUSSIONS

Our aim is to obtain B/Q values more accurately in different states of K atom so that they can be combined with the available precise experimental results for B to estimate Q . In order to verify the accuracies of B/Q results from our calculations, it would be felicitous to test the accuracies of the wave functions in the nuclear region. Owing to the fact that our calculation procedure deals with many numerical computations at different stages, along with that it correlates with higher excitations configurations indirectly, hence it would be very difficult to estimate uncertainties from the used numerical methods and approximations taken at the level of excitations. With the intention of verifying accuracies of the wave functions in the nuclear region, we have calculated A for many states in K. Assuming that the anomalous effects due to different nuclear sizes in all the considered isotopes are very small, we evaluate A/g_I in ^{39}K and determine A values for the corresponding isotopes using their respective g_I values. We have used experimental values of $g_I(^{39}\text{K}) = 0.2609772$, $g_I(^{40}\text{K}) = -0.324525$ and $g_I(^{41}\text{K}) = 0.1432467$ [9] to estimate these quantities ignoring their uncertainties as they will not meddle the results within the reported uncertainties. Both the calculated and experimental results are compared in Table II. We estimate uncertainties in our calculations by considering incompleteness of basis functions, contributions from the inactive orbitals in the RCC method, higher order excitation levels and from the neglected terms in the non-truncative series of Eq. (3.15). The upper limit to these uncertainties are given in the parentheses of the above table. Clearly, our estimated uncertainties are fair enough to compare with the available experimental results and our assumption for neglecting the anomalous effects for different isotopes seem to be reasonable.

We also compare our A results for ^{39}K obtained using DF, CCSD and CCSD(T) methods with another recent calculations [42] in Table III. In Ref. [42] Safronova and Safronova have also used linearized RCC method with singles and doubles approximation (SD method) and including important triples effects for some of the states (SDpT method). They find large differences between

their SD and SDpT results in contrast to our finding of small differences between our CCSD and CCSD(T) results. However, both the calculations reveal that the signs of the A values of the $3D_{5/2}$ and $5D_{5/2}$ states are negative, which were not resolved correctly in the measurements. Moreover, these calculations indicate that correlation effects in the considered atom are substantial for which an all order perturbative method like ours is suitable to determine wave functions accurately. To our knowledge, A values are not known experimentally for some of the states in ^{39}K and close agreement between the results from both the calculations in these states will be very useful to conduct new measurements in the right direction. Also, we have given A values for few excited states where neither measurements nor theoretical calculations are available.

Following A results, we present now our calculated B/Q results using the DF, CCSD and CCSD(T) methods in Table IV for the states where precise experimental B results for ^{39}K and ^{41}K are available. We also estimate the uncertainties associated with the results obtained using CCSD(T) method and present them in the parentheses of the same table. The uncertainties are estimated using the procedure as we followed for A . To justify that, trends of correlation effects for both the properties behave in a similar manner, we present contributions from various RCC terms to both A and B/Q results in Table V for few important states. It is found that, states where angular momentum is larger than half, the contributions from the correlation effects are always of similar scale in magnitude and the contributions coming from $\overline{O}S_{2v} + cc$ are larger than $\overline{O}S_{1v} + cc$. This implies that the core-polarization effects are large to estimate B/Q results in the considered atom which are accounted for, up to all orders through $\overline{O}S_{2v} + cc$ RCC terms in our calculations. There are no other calculated results for B/Q available to our knowledge in any of the considered isotopes of K to compare with our results.

Both the calculated results for A and B/Q seem to be very accurate, moreover A values are in good agreement with the available experimental results. There are also several experimental results available for B in ^{39}K as well as ^{41}K which are given in Table IV [1–3, 36, 38, 43]. The most precise values are quoted in bold fonts for the respective states in the same table and we combine these results with our calculated B/Q values to estimate Q s in these two isotopes. We obtain three different values of Q in ^{39}K and two values in ^{41}K . All these estimated values agree with each other in their respective uncertainties, but the most precise results which are obtained from the $4P_{3/2}$ state are $0.0625(17) b$ and $0.0744(10) b$ for ^{39}K and ^{41}K , respectively. Here we have used the following expression to evaluate the net uncertainties of Q values

$$\delta C = C \sqrt{\left(\frac{\delta A}{A}\right)^2 + \left(\frac{\delta B}{B}\right)^2}, \quad (4.1)$$

where we assume C is the extracted value from A/B and

TABLE II: Comparison of calculated and available experimental A results in $^{39-41}\text{K}$ (in MHz). Theoretical A s in different isotopes are evaluated using the calculated CCSD(T) results of A/g_I in ^{39}K and their respective experimental g_I values. Uncertainties estimated from the calculations are given in parentheses of our results.

State	This work			Experiment		
	^{39}K	^{40}K	^{41}K	^{39}K	^{40}K	^{41}K
$4S_{1/2}$	229.6(2.0)	-285.5(2.5)	126.0(1.1)	230.8598601(3)[3]	-285.7308(24)[3]	127.0069352(6) [3]
$4P_{1/2}$	27.4(5)	-34.04(62)	15.02(27)	27.775(42)[2] 28.85(30) [3] 27.80(15) [34] 27.5(4) [35] 28.859(15)[36]	-34.523(25)[2] -34.49(11)[34]	15.245(42) [2] 15.19(21) [34] 15.1(8) [35]
$4P_{3/2}$	5.9(2)	-7.35(37)	3.25(16)	6.093(25)[2] 6.06(8) [3] 6.00(10) [38] 6.13(5) [37]	-7.585(10)[2] -7.48(6) [34] -7.59(6) [39]	3.363(25)[2] 3.40(8) [37] 3.325(15) [40]
$3D_{3/2}$	1.0(2)	-1.25(25)	0.55(11)	0.96(4)[1]	1.07(2)[1]	0.55(3) [1]
$3D_{5/2}$	-0.57(5)	0.711(62)	-0.314(27)	0.62(4)[1]	0.71(4)[1]	0.40(2) [1]
$4D_{3/2}$	0.686(4)	-0.853(5)	0.377(2)			
$4D_{5/2}$	-0.332(2)	0.413(2)	-0.182(1)			
$5S_{1/2}$	55.0(1.0)	-68.4(1.2)	30.18(55)	55.50(60)[3]		
$5P_{1/2}$	8.8(5)	-10.98(62)	4.84(27)	9.02(17)[3]		
$5P_{3/2}$	1.9(2)	-2.37(25)	1.04(11)	1.969(13) [3] 1.95(5) [38]	-2.45(2) [3]	1.08(2) [3]
$5D_{3/2}$	0.39(5)	-0.489(62)	0.22(27)	0.44(10)[3]		
$5D_{5/2}$	-0.171(7)	0.213(9)	-0.094(4)	$\pm 0.24(7)$ [3]		
$6S_{1/2}$	21.1(6)	-26.24(75)	11.58(33)	21.81(18)[3]		12.03(40) [3]
$6P_{1/2}$	3.9(4)	-4.87(50)	2.15(22)	4.05(7)[3]		
$6P_{3/2}$	0.9(2)	-1.17(25)	0.51(11)	0.886(8)[3]		
$6D_{3/2}$	0.24(5)	-0.297(62)	0.131(27)	0.25(3)[41] $\pm 0.2(2)$ [3]		
$6D_{5/2}$	-0.112(5)	0.139(6)	-0.061(3)	-0.12(4)[41] $\pm 0.10(10)$ [3]		
$7S_{1/2}$	10.3(5)	-12.83(62)	5.66(27)	10.79(5)[3] $\pm 2.18(5)$ [3]		
$7P_{1/2}$	2.1(3)	-2.61(37)	1.15(16)			
$7P_{3/2}$	0.50(3)	-0.62(37)	0.28(16)			
$7D_{3/2}$	0.15(1)	-0.19(12)	0.083(5)			
$7D_{5/2}$	-0.068(5)	0.085(6)	-0.037(3)			
$8S_{1/2}$	5.8(2)	-7.27(25)	3.21(11)	5.99(8)[3]		
$8P_{1/2}$	1.3(1)	-1.56(12)	0.69(55)			
$8P_{3/2}$	0.301(5)	-0.374(6)	0.165(3)			
$8D_{3/2}$	0.101(2)	-0.126(2)	0.055(11)			
$8D_{5/2}$	-0.040(1)	0.050(1)	-0.022(1)			
$9S_{1/2}$	3.4(3)	-4.25(37)	1.88(16)			
$9P_{1/2}$	1.0(1)	-1.19(12)	0.53(55)			
$9P_{3/2}$	0.230(4)	-0.286(5)	0.126(2)			
$9D_{3/2}$	0.334(4)	-0.415(5)	0.183(2)			
$9D_{5/2}$	-0.148(2)	0.184(2)	-0.081(1)			
$10S_{1/2}$	2.2(3)	-2.68(37)	1.18(16)	2.41(5)[3]		

δA , δB and δC are their respective uncertainties.

Among both the new Q values in ^{39}K and ^{41}K , the relative uncertainty in Q of ^{41}K is small. Moreover there are also experimental results for the ratios of Q values between ^{39}K , ^{40}K and ^{41}K are available as [44, 46, 47]

$$\frac{Q(^{40}\text{K})}{Q(^{39}\text{K})} = -1.244 \pm 0.002 \quad (4.2)$$

and

$$\frac{Q(^{41}\text{K})}{Q(^{39}\text{K})} = 1.2173 \pm 0.0001. \quad (4.3)$$

Using the measured $\frac{Q(^{41}\text{K})}{Q(^{39}\text{K})}$ and Q value of ^{41}K , we get a new Q value for ^{39}K as 0.0612(8) b . Considering both the values of Q in ^{39}K , we restrict the lower and upper limits of $Q(^{39}\text{K})$ to 0.0608 b and 0.0620 b , respectively.

TABLE III: Comparison between different theoretical results of A in ^{39}K (in MHz).

State	Others [42]			This Work		
	DF	SD	SDpT	DF	CCSD	CCSD(T)
$4S_{1/2}$	146.91	237.40	228.57	146.794	229.573	229.556
$4P_{1/2}$	16.616	28.689	27.662	16.616	27.247	27.371
$4P_{3/2}$	3.233	6.213	5.989	3.234	5.886	5.913
$3D_{3/2}$	0.447	0.983	1.111	0.447	1.006	1.003
$3D_{5/2}$	0.192	-0.535	-0.639	0.192	-0.574	-0.572
$4D_{3/2}$	0.281	0.678		0.281	0.690	0.686
$4D_{5/2}$	0.120	-0.307		0.120	-0.334	-0.332
$5S_{1/2}$	38.877	56.102	54.817	38.847	55.070	54.981
$5P_{1/2}$	5.735	9.202	8.949	5.735	8.755	8.827
$5P_{3/2}$	1.117	1.988	1.932	1.117	1.887	1.903
$5D_{3/2}$	0.168	0.409		0.168	0.396	0.393
$5D_{5/2}$	0.072	-0.167		0.072	-0.173	-0.171
$6S_{1/2}$	15.759	22.025	21.609	15.105	21.167	21.10
$6P_{1/2}$	2.629	4.066	4.014	2.629	3.874	3.918
$6P_{3/2}$	0.512	0.874	0.866	0.512	0.928	0.937
$6D_{3/2}$	0.105	0.253		0.104	0.241	0.239
$6D_{5/2}$	0.0448	-0.0975		0.045	-0.113	-0.112
$7S_{1/2}$	7.900	10.876	10.690	7.894	10.363	10.317
$7P_{1/2}$	1.417	2.191	2.140	1.417	2.066	2.095
$7P_{3/2}$	0.276	0.473	0.462	0.276	0.495	0.502
$7D_{3/2}$	0.0685	0.1644		0.067	0.154	0.152
$7D_{5/2}$	0.0293	-0.0611		0.028	-0.069	-0.068
$8S_{1/2}$	4.511	6.156	6.057	4.536	5.880	5.847
$8P_{1/2}$				0.855	1.236	1.257
$8P_{3/2}$				0.166	0.296	0.301
$8D_{3/2}$				0.048	0.102	0.101
$8D_{5/2}$				0.019	-0.040	-0.040
$9S_{1/2}$	2.814	3.818	3.759	2.685	3.444	3.420
$9P_{1/2}$				0.695	0.945	0.958
$9P_{3/2}$				0.136	0.227	0.230
$9D_{3/2}$				0.189	0.338	0.334
$9D_{5/2}$				0.083	-0.151	-0.148
$10S_{1/2}$	1.871	2.529	2.491	1.878	2.171	2.154

TABLE IV: Calculated B/Q values (in MHz/ b) from our DF, CCSD and CCSD(T) methods and accurately known experimental B results (in MHz) in ^{39}K and ^{41}K . The most precise B results are given in bold fonts and Q values are estimated by combining these results with the calculated B/Q values in both the isotopes.

State	Theory			Experiment $B(^{39}\text{K})$	$Q(^{39}\text{K})$	Experiment $B(^{41}\text{K})$	$Q(^{41}\text{K})$
	DF	CCSD	CCSD(T)				
$4P_{3/2}$	23.000	44.392	44.6(5)	2.786(71) [2] 2.72(12) [36] 2.83(13) [43] 2.9(2) [38]	<u>0.0625(17)</u>	3.351(71) [2] 3.34(24) [37] 3.320(23) [40]	<u>0.0744(10)</u>
$5P_{3/2}$	7.866	13.833	13.9(4)	0.870(22) [3] 0.92(10) [38]	0.0626(22)	1.06(4) [37]	0.0763(36)
$6P_{3/2}$	3.340	6.285	6.4(5)	0.370(15) [3]	0.0578(51)		

Therefore, we recommend Q value of ^{39}K as 0.0614(6) b . Now with this most precise Q value and the above ratios of Q values between different isotopes, we get precise Q values for ^{40}K and ^{41}K as -0.0764(8) b and 0.0747(7) b , respectively. There are also other reported Q values which we have compared them with ours in Table VI. As seen from the table, there are three other works re-

port these results [11, 12, 44]. Apart from Ref. [44], the calculations carried out in these works are rigorous and results reported in [12] are the latest. Q values reported in [11] matches with our estimated values with some overlaps within the predicted uncertainties, however results reported in [12] disagree with us. In both these theoretical works, they have determined electric field gradients at

TABLE V: Contributions from different RCC terms to A (in MHz) and B/Q (in MHz/b), whereas c.c. stands for complex conjugation.

State	\bar{O}		$\bar{O}S_{1v} + c.c.$		$\bar{O}S_{2v} + c.c.$		Others		Norm	
	A	B/Q	A	B/Q	A	B/Q	A	B/Q	A	B/Q
$4S_{1/2}$	146.576		46.148		33.0457		6.707		-2.920	
$4P_{1/2}$	16.341		5.500		4.820		0.900		-0.190	
$4P_{3/2}$	3.186	22.662	1.062	7.562	1.430	13.386	0.275	1.280	-0.040	-0.305
$3D_{3/2}$	0.464	1.168	0.430	1.080	-0.059	2.947	0.185	0.089	-0.017	-0.090
$3D_{5/2}$	0.199	1.666	0.183	1.527	-0.766	4.223	-0.178	0.127	0.010	-0.128
$5S_{1/2}$	38.770		7.898		8.200		0.725		-0.612	
$5P_{1/2}$	5.683		1.535		1.571		0.100		-0.062	
$5P_{3/2}$	1.089	7.752	0.296	2.114	0.463	3.967	0.068	0.206	-0.013	-0.096
$6S_{1/2}$	15.043		2.882		3.150		0.246		-0.217	
$6P_{1/2}$	2.615		0.633		0.630		0.067		-0.027	
$6P_{3/2}$	0.510	3.631	0.122	0.872	0.276	1.825	0.037	0.070	-0.006	-0.043
$7S_{1/2}$	7.902		1.148		1.309		0.062		-0.104	
$8S_{1/2}$	4.540		0.592		0.746		0.026		-0.057	
$9S_{1/2}$	2.687		0.316		0.438		0.011		-0.032	
$10S_{1/2}$	1.880		0.013		0.291		-0.014		-0.015	

TABLE VI: Reported values of nuclear quadrupole moments Q in b for ^{39}K , ^{40}K and ^{41}K from various studies.

Isotope	This work	Others
^{39}K	0.0614(6)	0.0585 ^a [12] 0.0601(15) [11] 0.049(4) [44]
^{40}K	-0.0764(8)	-0.073 ^a [12] -0.0749(19) [11]
^{41}K	0.0747(7)	0.0711 ^a [12] 0.0733(18) [11]

^aAccuracy is expected to be better than 1 percent

the nucleus to extract the nuclear quadrupole moments and the results are model independent. But both the calculations are less rigorous than the present calculations. In Ref. [11], Sundholm and Olsen have used a non-relativistic large scale finite-element multi-configuration Hartree-Fock configuration interaction (MCHF) method. The core contributions were estimated from the core-valence correlation calculations and the relativistic corrections are accounted separately from the DF calculation. Contrast to this work, we have considered the core correlation and core-valence correlations to all orders and relativistic effects are included to all orders through the RCC method. In fact, their truncative CI method is known to have size-consistent problem [48] against our RCC method. On the other-hand, level of approximations employed to carry out calculations in Ref. [12] by Kellö and Sadlej are comparable to the present work. In their work, calculations are performed with a scalar relativistic Hamiltonian using Douglas-Kroll approach and CCSD(T) method is used to account the correlation ef-

fects. Since this approach is better than the above MCHF method, the results reported in [12] were considered to be more accurate and estimated to be within 1% accuracy. However, we find the reported values in [12] are smaller in magnitudes as compared to our estimations.

It will be interesting to see further theoretical studies of B/Q results to draw comparison with the present work. Further, we combine our calculated B/Q results with the newly obtained Q values to determine theoretical results for B in many states of the considered isotopes of K. These results are given in Table VII. We have also neglected here the anomalous effects in calculated B/Q values for different isotopes due to their negligible roles. If some of these B results can be measured more precisely than the reported results, then combining those results with our calculated B/Q values will definitely give rise better Q values in these isotopes. In fact, more precise theoretical calculations of B/Q results in these isotopes can also give rise to more accurate Q values in K.

As can be noticed in Table VII, our estimated B results for different states in K isotopes agree very well in most of the states except with the $3D$ states. We suggest to carry out further measurements of B in these states to ascertain our results. Theoretical results for B are also given in many excited states for the first time which can be verified by the future measurements.

V. CONCLUSION

We have employed relativistic coupled-cluster method to calculate matrix elements of the hyperfine interaction Hamiltonians in potassium atom. By performing calculations of the magnetic dipole hyperfine structure constants in this atom, we have tested the accuracies of the wave

TABLE VII: Comparison of estimated and experimental B results in $^{39-41}\text{K}$ (in MHz).

State	$(B/Q)^{(Th)}$	This Work			Experiments		
		^{39}K	^{40}K	^{41}K	^{39}K	^{40}K	^{41}K
$4P_{3/2}$	44.6(5)	2.738(41)	-3.41(5)	3.332(49)	2.786(71)[2] 2.9(2) [38] 2.72(12) [37] 2.83(13) [3]	-3.445(90) [2] -3.23(50)[34] -3.5(5)[39]	3.351(71)[2] 3.34(24) [37] 3.320(23)[40]
$3D_{3/2}$	5.2(5)	0.319(31)	-0.40(4)	0.388(38)	0.37(8) [1]	0.4(1) [1]	0.51(8)[1]
$3D_{5/2}$	7.4(4)	0.454(25)	-0.565(31)	0.553(30)	<0.3 [1]	0.8(8)[1]	< 0.2 [1]
$4D_{3/2}$	2.35(4)	0.144(3)	-0.180(4)	0.176(3)			
$4D_{5/2}$	3.35(4)	0.206(3)	-0.256(4)	0.250(4)			
$5P_{3/2}$	13.9(4)	0.853(26)	-1.06(3)	1.038(31)	0.870(22) [37, 38] 0.92(10)[38]	-1.16(22)[39]	1.06(4) [37]
$5D_{3/2}$	1.16(8)	0.071(5)	-0.088(6)	0.087(6)			
$5D_{5/2}$	1.65(10)	0.101(6)	-0.126(8)	0.123(8)			
$6P_{3/2}$	6.4(5)	0.393(31)	-0.489(39)	0.478(38)	0.370(15)[45]		
$6D_{3/2}$	0.72(5)	0.044(3)	-0.055(4)	0.054(4)	0.05(2) [41]		
$6D_{5/2}$	1.02(6)	0.063(4)	-0.078(5)	0.076(5)			
$7P_{3/2}$	3.4(3)	0.209(19)	-0.260(23)	0.254(23)			
$7D_{3/2}$	0.44(3)	0.027(2)	-0.034(2)	0.033(2)			
$7D_{5/2}$	0.62(4)	0.038(2)	-0.047(3)	0.046(3)			
$8P_{3/2}$	2.0(2)	0.123(12)	-0.153(15)	0.149(15)			
$8D_{3/2}$	0.29(2)	0.018(1)	-0.022(2)	0.022(2)			
$8D_{5/2}$	0.36(2)	0.022(1)	-0.028(2)	0.027(2)			
$9P_{3/2}$	1.5(2)	0.092(12)	-0.115(15)	0.112(15)			
$9D_{3/2}$	0.92(6)	0.056(4)	-0.070(5)	0.069(5)			
$9D_{5/2}$	1.35(8)	0.083(5)	-0.103(6)	0.101(6)			

functions in the nuclear region. These wave functions were further used for the electric quadrupole hyperfine interaction studies. By combining our calculations with the corresponding measurements, we obtained the nuclear quadrupole moments as 0.0614(6) b , -0.0764(8) b and 0.0747(7) b for ^{39}K , ^{40}K and ^{41}K , respectively. These results agree with one of the previous work but do not agree with others including the latest reported results. After obtaining nuclear quadrupole moments, we substituted them to obtain electric quadrupole hyperfine structure constants in many states and found very good agree-

ment with the experimental results except for the $3D$ states. Also, we have given some of the results that were not reported earlier. We suggest further studies of the considered properties to ascertain our results.

VI. ACKNOWLEDGMENT

Computations were carried out using 3TFLOP HPC cluster of Physical Research Laboratory, Ahmedabad.

-
- [1] A. Sieradzan, R. Stoleru, W. Yei and M. D. Havey, Phys. Rev. A **55**, 3475 (1997).
 - [2] S. Flake, E. Tiemann, C. Lisdat, H. Schnatz, and G. Grosche, Phys. Rev. A **74**, 032503 (2006).
 - [3] E. Arimondo, M. Inguscio, and P. Violino, Rev. Mod. Phys. **49**, 31 (1977).
 - [4] B. K. Sahoo, G. Gopakumar, R. K. Chaudhuri and B. P. Das, Phys. Rev. A **68**, 040501(R) (2003).
 - [5] B. K. Sahoo, R. K. Chaudhuri, B. P. Das, H. Merlitz and D. Mukherjee, Phys. Rev. A **72**, 032507 (2005).
 - [6] H. S. Nataraj, B. K. Sahoo, B. P. Das and D. Mukherjee, Phys. Rev. Lett. **106**, 200403 (2011).
 - [7] B. K. Sahoo, Phys. Rev. A **73**, 062501 (2006).
 - [8] B. K. Sahoo, Phys. Rev. A **80**, 012515 (2009).
 - [9] N. J. Stone, *Table of Nuclear Magnetic Dipole and Electric Quadrupole Moments*, IAEA Nuclear Data Section, Vienna International Centre, 1400 Vienna, Austria, April 2011.
 - [10] G. W. Series, Phys. Rev. **105**, 1128 (1957).
 - [11] Dage Sundholm, Jeepe Oslen, J. Chem. Phys. **98**, 9 (1993).
 - [12] Vladimir Kellö, Andrzej J. Sadlej, Chemical Physics Letters **292**, 403-410 (1998).
 - [13] <http://www.webelements.com/potassium/nmr.html>
 - [14] K. Blaum, W. Geithner, J. Lassen, P. Lievens, K. Marinova and R. Neugart, CERN-PH-EP/2007-038 (2007).
 - [15] G. Neyens, Rep. Prog. Phys. **66**, 633 (2003).
 - [16] B. T. Feld, *Nuclear electric quadrupole moments and*

- quadrupole couplings in molecules*, Nuclear Science Series, National Research Council (1949).
- [17] L. A. Errico and M. Rentera, Phys. Rev. B **73**, 115125 (2006).
 - [18] K. Asahi and K. Matsuta, Nucl. Phys. A **693**, 63 (2001).
 - [19] G. Martinez-Pinedo, P. Schwerdtfeger, E. Caurier, K. Langanke, W. Nazarewicz, and T. Sohnel, Phys. Rev. Lett. **87**, 062701 (2001).
 - [20] C. Schwartz, Phys. Rev. **97**, 380 (1955).
 - [21] K. T. Cheng and W. J. Childs, Phys. Rev. A **31**, 2775 (1985).
 - [22] A. R. Edmonds, *Angular Momentum in Quantum Mechanics*, Princeton University Press, USA (1996).
 - [23] P. J. C. Aerts and W. C. Nieuwpoort, Chem. Phys. Letters, **113**, 165 (1985).
 - [24] O. Visser, P. J. C. Aerts, D. Hegarty and W. C. Nieuwpoort, Chem. Phys. Letters, **134**, 34 (1987).
 - [25] A. Mohanty and E. Clementi, in Kinetically Balanced Geometric Gaussian Basis Set Calculations For Relativistic Many Electron Atoms, Modern Techniques in Computational Chemistry: MOTEC-89, edited by E. Clementi (ESCOM, Leiden, 1989), **Chap. 4**, p. 169.
 - [26] Richard E. Stanton and Stephen Havriliak, J. Chem. Phys. **81**, 1910 (1984).
 - [27] P. Ragavan, At. Data Nucl. Data Tables, **42**, 189 (1969).
 - [28] I. Lindgren, Int. J. Quantum Chem. **12**, 33 (1978).
 - [29] D. Mukherjee and S. Pal, Adv. Quantum Chem. **20**, 281 (1989).
 - [30] U. Kaldor, J. Chem. Phys. **87**, 467 (1987); **87**, 4693 (1987).
 - [31] B. K. Sahoo, C. Sur, T. Beier, B. P. Das, R. K. Chaudhuri, and D. Mukherjee, Phys. Rev. A **75**, 042504 (2007).
 - [32] B. K. Sahoo, G. Gopakumar, R. K. Chaudhuri, B. P. Das, H. Merlitz, U. S. Mahapatra and D. Mukherjee, Phys. Rev. A **68**, 040501(R) (2003).
 - [33] B. K. Sahoo, R. K. Chaudhuri, B. P. Das, S. Majumder, H. Merlitz, U. S. Mahapatra, and D. Mukherjee, J. Phys. B **36**, 1899 (2003).
 - [34] N. Bendali, H. T. Duong, and J. L. Vialle, J. Phys. B **14**, 4231 (1981).
 - [35] F. Touchard, P. Guimbal, S. Buttgenbach, R. Klapisch, M. De Saint Simon, J. M. Serre, C. Thibault, H. T. Duong, P. Juncar, S. Limberman, J. Pinard, and J. L. Vialle, Phys. Lett. B, **108**, 169 (1982).
 - [36] A. Banerjee, D. Das, and V. Natarajan, Opt. Lett. **28**, 1579 (2003).
 - [37] J. Ney, R. Repnow, H. Bucke, and G. Schatz, Z. Phys. **213**, 192 (1968).
 - [38] Robert W. Schmieder, Allen Lurio and W. Happer, Phys. Rev. **76**, 173 (1968).
 - [39] J. Ney, Z. Phys. **223**, 126 (1969).
 - [40] A. Sieradzian, A. Lurio, and W. Harper, Phys. Rev. **173**, 76 (1968).
 - [41] M. Glódz and M. Krańska-Miszczak, J. Phys. B **18**, 1515 (1985).
 - [42] U. I. Safronova and M. S. Safronova, Phys. Rev. A **78**, 052504 (2008).
 - [43] P. Risberg, Ark. Fys. **10**, 583 (1956).
 - [44] R. M. Sternheimer and R. F. Peierls, Phys. Rev. A **3**, 837 (1971).
 - [45] S. Savanberg, Phys. Scr. **4**, 475 (1971).
 - [46] P. A. Bonczyk and V. W. Hughes, Phys. Rev. **161**, 15 (1967).
 - [47] E. P. Jones and S. R. Hartmann Phys. Rev. B **6**, 757771 (1972).
 - [48] A. Szabo, N. S. Ostlund, *Modern Quantum Chemistry*, Dover Publication (1982).